# Reactive Power Control of a Direct Grid Connected Slip Synchronous Permanent Magnet Wind Generator

Andries T. Spies, Maarten J. Kamper
Department of Electrical and Electronic Engineering
Stellenbosch University
Private Bag X1, Matieland, 7602, South Africa

*Abstract* – **In this paper a possible reactive power control method is developed for the direct-drive direct-grid connected slip permanent magnet wind generator. By using a solid-state-assisted on-load tap changer transformer, the terminal voltage of the generator can be varied. In this way the generator can be operated in over- or under-excited mode, allowing for discreet control over the reactive power output of the generator. Solid-state switches are used in the transformer switchgear to increase the lifetime of the diverter circuit. Along with the transformer, two small capacitor banks are also used to deliver additional reactive power when needed. The performance of the system is simulated and the results are evaluated against the grid code specifications of the National Energy Regulator of South Africa.**

*Index Terms* – **direct-drive; grid connection; permanent magnet; wind generator; on-load tap changer; reactive power control.**

## I. Introduction

ECONOMIC development requires abundant amounts of electrical energy. Unfortunately traditional means of generating the required electrical power are not sustainable. Of all the endeavours that are providing sustainable electrical energy, wind power seems to stand out as a main contender. Although wind has been used as a power source for more than a thousand years, technology is still being developed to improve efficiency and lower the cost and maintenance of the generator systems.

### A. Doubly Fed Induction Wind Generators

The bulk of today's wind farms use the doubly fed induction generator (DFIG) setup as shown in Fig. 1. The stator is connected to the grid, while the rotor is connected through a solid-state power converter (SSC) that controls the frequency of the wound rotor. The power converter also performs reactive power compensation and allows for smooth grid connection [1]. According to [2] and [3] power converters, after gearboxes and hydraulics, are listed as one of the main reasons for wind turbine failure.

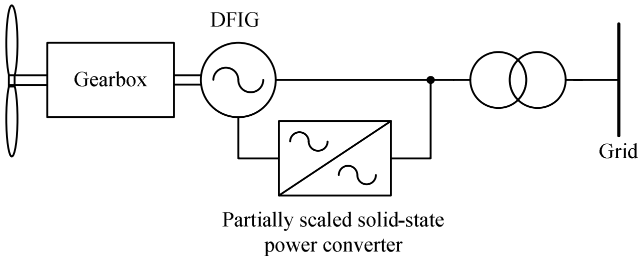


Fig. 1. DFIG with a partially rated power converter [1].

### B. Slip Synchronous Permanent Magnet Wind Generator

The slip synchronous permanent magnet (PM) generator (SSG) was developed to alleviate the need for heavy and expensive gearboxes and expensive SSCs. This direct turbine drive PM generator allows for a direct grid connectable system, which is less complex and more cost effective. As shown in Fig. 2, the SSG consists of an induction generator (IG) cage magnetically coupled to a common free rotating PM rotor. The PM rotor is also magnetically coupled to the stator of a synchronous generator (SG). The IG-cage is directly connected to the turbine blades i.e. without the use of a gearbox. The SG-stator on the other hand is directly connected to the grid; hence the SG operates at synchronous speed.

Fig. 3 shows a single-line diagram of the SSG wind generator connected to the grid via a tapped transformer. Details regarding the design, modelling and grid connection of the SSG are given in [4]. In this study the focus is on the use of a SSG rated at 15 kW and 1000 Nm torque.

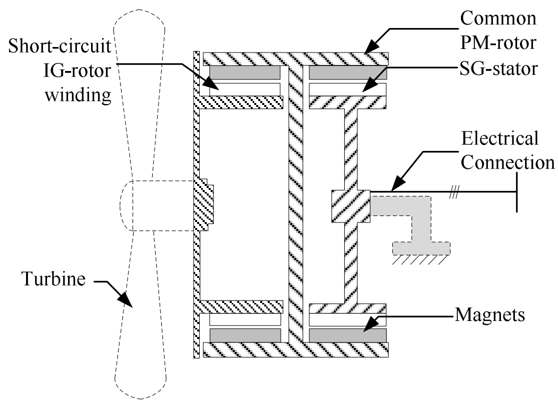


Fig. 2. Cross-section side view showing the components of the SSG.

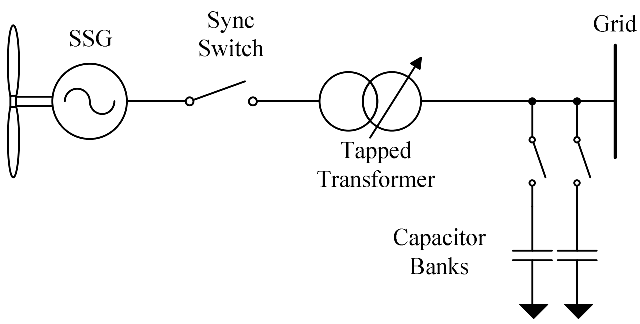


Fig. 3. SSG wind turbine generator connected to the grid via a synchronisation switch and an on-load tap changer transformer with shunt capacitor banks to provide reactive power compensation.

978-1-4673-4569-9/13/$31.00  

## II. GRID CODE SPECIFICATIONS

Integrating wind farms with the electrical grid tends to introduce voltage instability due to the uncontrollable nature of the energy source. As the wind speed varies at irregular intervals, the output generated power and current change. This causes the voltage at the point of common connect (PCC) to fluctuate. Since wind power generation plants are often situated in rural areas, relatively large voltage variations at the PCC are of huge concern [5].

Due to these problems various national energy regulators in the world have specific technical standards regarding the connection requirements for wind energy facilities (WEF). The technical requirements can be divided into five categories namely: frequency, voltage, power factor control, active power curtailment and low voltage ride through.

For this study the requirements as specified by the National Energy Regulator of South Africa (NERSA) are used. The intention is to design and evaluate the use of a solid-state-assisted on-load tap changer transformer to control the excitation mode of the SSG.

### A. *Reactive Power Control Requirement*

The grid code has strict requirements regarding the reactive power control capability of a WEF. Fig. 4 shows the required continuous operating region for a WEF smaller than 20 MW [6]. A WEF with rated active power of less than 20 MW must be able to constantly supply a reactive power output of not less than 0.975 lagging and 0.975 leading, available at the PCC. This reactive power must be available from minimum generation to full-rated active power and must be fully variable between these limits.

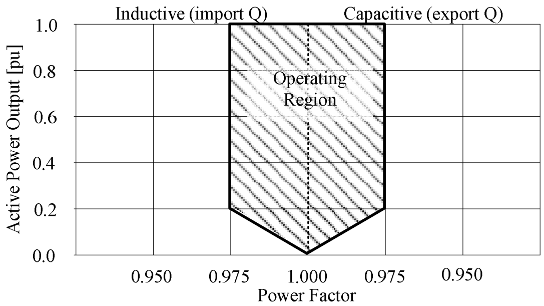


Fig. 4. Reactive power requirement for a WEF smaller than 20 MW [6].

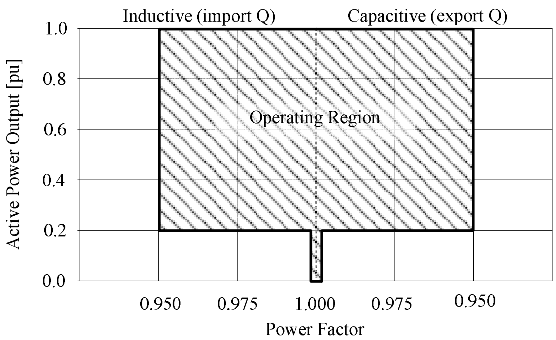


Fig. 5. Reactive power requirement for a WEF larger than 20 MW [6].

A WEF with rated active power of more than 20 MW must be designed to constantly supply reactive power of not less than 0.95 lagging and 0.95 leading, at the PCC. This reactive power shall also be available throughout the power range of the generator, as shown in Fig. 5 [6]. It is important to note that a WEF is not allowed to import any reactive power during generator start up [6].

## III. ON LOAD TAP CHANGER DESIGN

Power transformers are used to step-up the voltage of the WEF at the PCC. Fig. 6 shows the circuit diagram of a classic on-load tap changer (OLTC) transformer. The switchgear is divided into two parts. The first part is called the selector circuit. The selector switch only pre-selects the next tap, and is never required to operate when current is flowing through the switch. The second part is called the diverter circuit. This circuit normally consists of four spring operated mechanical switches that operate in a specific order. The switches are responsible for diverting the load current between the selected transformer taps.

Due to the fact that current is "broken" by the diverter switches, arcing occurs, leading to heavy contact wear that limits the operational life of the diverter subsystem [7]. Due to the uncontrollable nature of the wind, various tap changes may be necessary per day, or even per hour. This will lead to short maintenance intervals and increased downtime for the WEF.

### A. *Solid-State-Assisted OLTC Transformer*

Due to the inherent disadvantages of mechanical switches, various hybrid OLTC systems have been considered. Hybrid OLTCs use both solid-state and mechanical switches, to respectively reduce arcing and conduction losses.

The simplest hybrid OLTC is one where the mechanical diverter switches are replaced by two solid-state switches as shown in Fig. 7. By substituting the mechanical switches in the diverter, all arcing is eliminated. With no arcing there will be a considerable reduction in transformer oil contamination, which is associated with contact wear due to electrical arcing. Since there are also no inter-tap currents the inter-tap resistors can be removed.

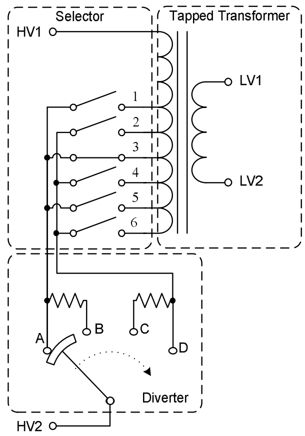


Fig. 6. Per phase circuit of the classic on-load tap changer [7].

Solid-state switches suffer from conduction power losses; which can be circumvented by using a bypass mechanical switch in parallel with the solid-state switch as shown in Fig. 7. Note the differences in the diverter subsystems of Fig. 6 and Fig. 7. Tests done on solid-state-assisted tap changers showed an 75 time improvement in the lifetime of the mechanical switch compared to the mechanical switch without bypass thyristors [8].

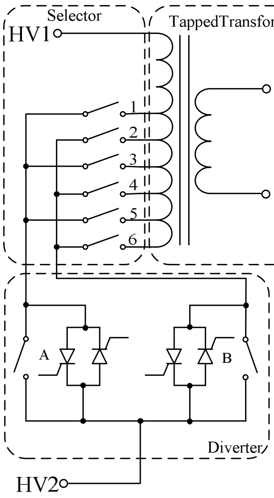


Fig. 7. Per phase solid-state assisted mechanical diverter circuit.

### B. Tap-changing simulation results

The working of the solid-state-assisted OLTC, in Fig. 7, is simulated using the Mentor Graphics SystemVision (MGSV) package. The modelling parameters used during the simulations are given in the Appendix. The control simulated signals for thyristor A and B and bypass switch B is shown in Fig. 8.

Consider that the generator is initially connected to the grid via tap 3 and switch A. When the controller receives the instruction to increase the voltage, tap 4 is closed with tap 3 still closed. The gate of thyristor A is set to high at 70 ms in Fig. 8, switch A opens at time 80 ms and thyristor A starts to conduct the load current. The diverter circuit is now ready to make a tap change. At time 95 ms the controller gives the thyristors the commands as shown in Fig. 8. The thyristors are now ready to exchange the load current. When the current in Fig. 9 goes through zero (at 99 ms) thyristor A stops conducting. When the voltage in Fig. 10 goes through zero (at 100 ms) thyristor B starts conducting. The simulated voltage spikes in Fig. 10 are caused by the current and the voltage not being perfectly in phase. This is due to the load being relatively inductive. These voltage spikes only occur when the thyristors are conducting.

At any time after thyristor B starts conducting, bypass switch B may be closed. For this simulation bypass switch B is closed at time 125 ms, as shown in Fig. 8 and Fig. 10. When the bypass switch closes, thyristor B stops conducting current. This concludes the tap switching operation.

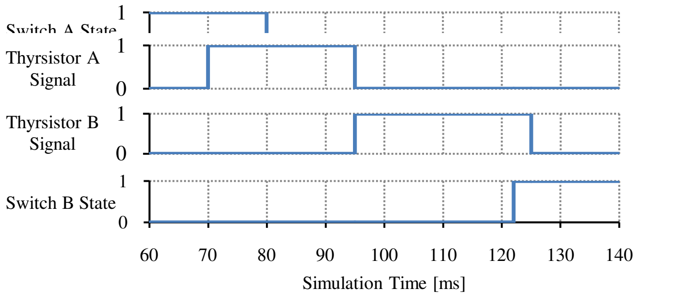


Fig. 8. Simulated control signals of thyristor A and B and bypass switch B of Fig. 7.

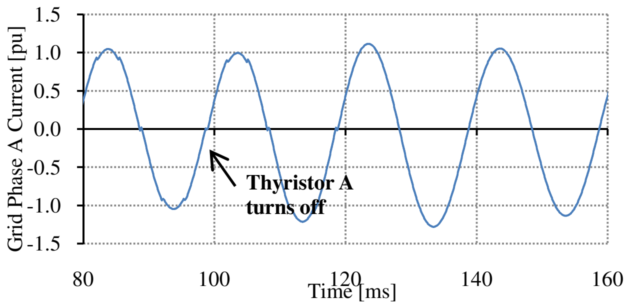


Fig. 9. Simulated phase current waveform during switching.

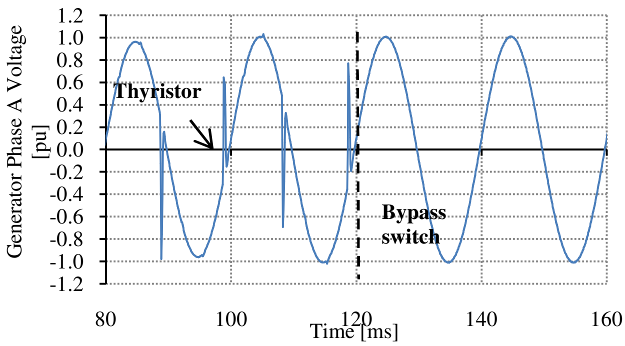


Fig. 10. Simulated phase voltage waveform during switching.

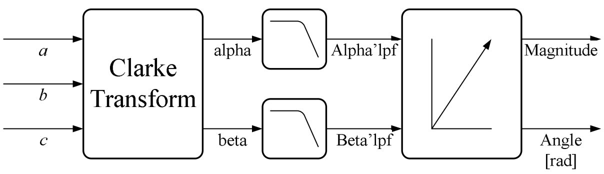


Fig. 11. Block diagram for calculating the current and voltage vector magnitude and angle.

### C. Simulation to determine switching transients

The current transients associated with changing the terminal voltage on the 15 kW SSG is simulated using the parameters as given in the Appendix. Throughout this simulation rated torque is applied to the SSG. At 2.5 seconds a tap change occurs and decreases the terminal voltage of the generator by 0.05 pu.

In the simulation the controller measures the three-phase voltage and current waveforms, and using the basic algorithm as shown in Fig. 11, the angle and magnitude of the current and voltage vectors are determined. The current overshoot, as shown in Fig. 12, is determined to be 0.11 pu with a 5% settling time of 40 ms.

## IV. Reactive Power Control

The SSG reacts in the same manner as a PMSG when seen from the grid. When the terminal voltage of the generator is changed the generator acts in the same manner as a SG when the excitation is changed. Fig. 13 shows a phasor diagram for the SSG. Since the generator uses permanent magnets to generate the field, the induced voltage ($E_A$) is near constant for all operating conditions. As can be seen in Fig. 13, when the terminal voltage ($V_\varphi$) is decreased; the generator operates as an over-excited SG (lagging current) and delivers reactive power. The opposite is true when the terminal voltage is increased; the generator then absorbs reactive power (leading current).

As long as the voltage at the PCC is within the required voltage region, as specified by the system operator, this method of controlling the reactive power can be achieved using the OLTC. Using the mathematic *dq*-model as explained in [9] the 15 kW SSG is simulated with the MGSV package. The power factor change is shown in Fig. 14 for various terminal voltages at different power values.

Although the generator model used during these simulations takes only the copper losses into account, it is apparent from Fig. 15 that changing the terminal voltage has a negative effect on the efficiency of the generator. The simulated efficiency and power factor at rated power are shown in Fig. 15. At rated power, the SSG absorbs reactive power when the terminal voltage is higher than 0.8 pu.

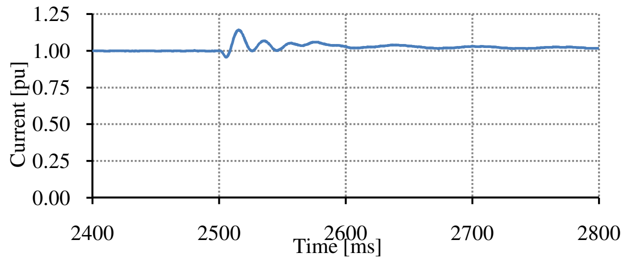


Fig. 12. Current vector magnitude response due to terminal voltage change at rated applied turbine torque.

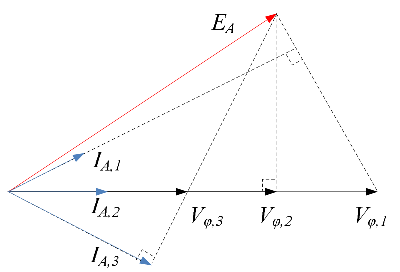


Fig. 13. Phasor diagram for different terminal voltages of the SSG.

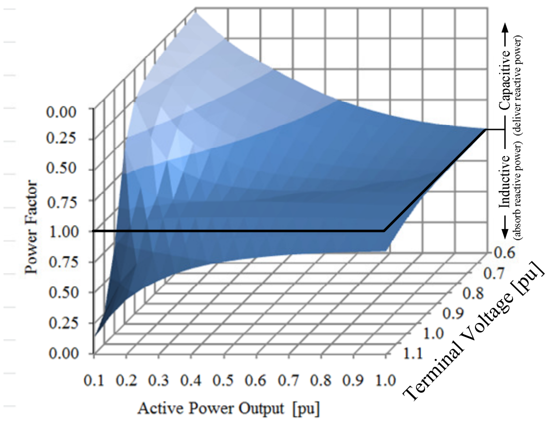


Fig. 14. Power factor angle of the SSG for variable power and terminal voltage.

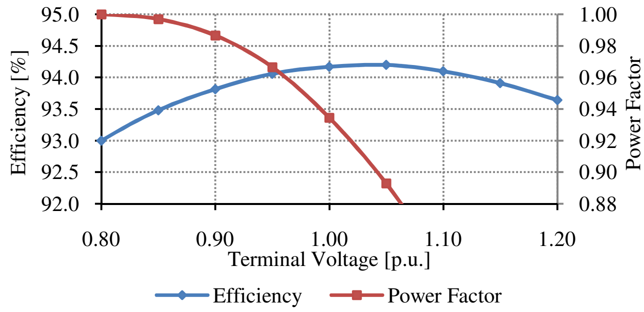


Fig. 15. Efficiency and power factor versus terminal voltage of the SSG at rated power.

### A. *Reactive power control simulation using only the OLTC*

Using the OLTC to control the reactive power output of the 15 kW SSG, is simulated using MGSV. The SSG is connected to a 400 V bus with grid line impedance values as determined by [4]. The turbine torque applied to the SSG-model during the simulation is linearly increased from zero to rated torque. The controller measures the current and voltage at the PCC and then changes the generator terminal voltage, using the OLTC, in such a way that the power factor angle is at or near zero, i.e. at unity power factor.

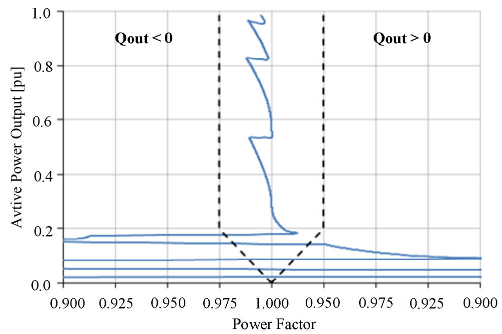


Fig. 16. Simulated power factor when using the OLTC to control the reactive output power of the generator for increasing active power values.

Fig. 16 shows the change in power factor with the change in active power output due to the applied turbine torque. At low power levels the difference in power factor between the different taps is very large. In this case the controller is unable to control the power factor at power levels below 0.2 pu.

### *B. Reactive power control simulation using the OLTC with capacitor banks*

Wind farms commonly use fixed shunt connected capacitor banks rated to compensate for reactive power at maximum power output. Capacitor banks are regarded as the easiest and cheapest method of providing reactive power, however they have disadvantages when compared to both Static VAR compensators (SVC) and the Static Synchronous Compensator (STATCOM). Because the reactive power delivered by capacitors is very voltage dependant ($Q_c = \omega C V^2$) they cannot provide voltage support. Switching multiple capacitor banks also causes voltage transients. It is also possible for a capacitor bank to aggravate harmonic content in the power system [10], [11].

By using two capacitor banks as shown in Fig. 3, three switching states are possible, either one of the capacitor banks can be connected, or the two banks are connected in parallel. This increases the reactive power control capability of the system shown in Fig. 3.

From the previous simulation it can be seen that with a tap change the reactive power output of the SSG changes by roughly 1700 var. By sizing the first capacitor bank to deliver a quarter (425 var) and the second capacitor bank a half (850 var) of the required reactive power, three additional discreet reactive power states are possible between each consecutive tap change.

For the simulation using the capacitors, the same turbine torque signal as used in the previous simulations is applied to the SSG model. The simulated results are compared to those when using only the tap changer. The controller is programmed to deliver unity power factor. When comparing Fig. 16 and Fig. 17 we can see an improvement in the reactive power control. In both cases there is a problem controlling the reactive power at very low active power levels.

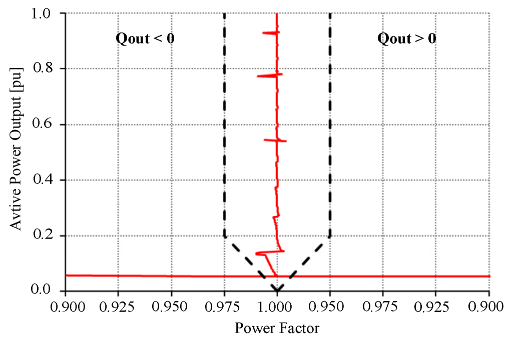


Fig. 17. Simulated power factor using the OLTC and the capacitor banks for increasing active output power.

During the simulation it can be seen that the controller jitters at some power levels. This can be seen in Fig. 17 at 0.55, 0.78 and 0.92 pu active power. At these power levels the controller is currently unable to select the proper capacitor-tap combination. This can be rectified by increasing the hysteresis bandwidth.

## V. Testing the OLTC

The reactive power control using an OLTC transformer is also experimentally investigated. The 15 kW SSG is driven by a 45 kW geared induction motor, which in turn is fed by a 37 kW Allen-Bradley variable speed drive. The SSG is connected to the grid via a manual synchronisation switch and an OLTC transformer implementing a solid-state assisted mechanical diverter circuit. The tapped transformer used has a power rating of 30 kW. Each consecutive transformer tap varies the generator voltage by approximately 0.03 pu.

### *A. Voltage and current transients present during tap changes*

The generator per phase voltage and line current are measured during a tap change operation while the generator is operating at rated power. Fig. 18 shows the small decrease in terminal voltage with the tap change, without interrupting the line current. The lack of voltage spikes is noted when comparing the voltage waveform in Fig. 18 with the simulated waveform in Fig. 10.

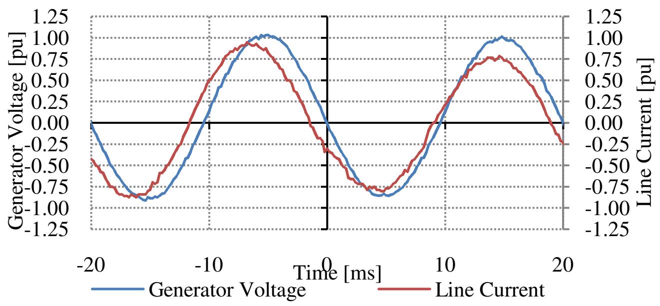


Fig. 18. Measured generator per phase voltage and line current during a tap change, decreasing the terminal voltage by 0.03 pu at time zero.

### *B. Reactive power control using the OLTC*

The use of the OLTC to control the power factor is also tested. The OLTC controller is set to maintain unity power factor as the active power is varied in the test. The no-operation bandwidth is selected as 1.0 kvar in test 1 and decreased to 0.6 kvar in test 2. The measured result of Fig. 21 compares, to a certain extent, well with the simulated results of Fig. 16. Again, the results of Fig. 19 the controller is unable to control the power factor at low active power values. At higher power values (>0.2 pu) the controller was able to keep the power factor near unity.

## VI. Conclusion

This paper details the proposed method of controlling the reactive power output of the direct-drive direct-grid connected SSG wind generator. The proposed method entails of using a solid-state-assisted on-load tap changer transformer to control the generator terminal voltage and thus the excitation mode of the permanent magnet generator.

From both the simulation and practical results it is found that the OLTC, implementing a solid-state assisted mechanical diverter circuit, can control the reactive power output of the generator without interrupting the load current. Due to the large change in reactive power output per tap change it is found that the controller is unable to control the power factor at power levels below 0.2 pu.

The use of two small capacitor banks to provide additional reactive power between consecutive tap changes is evaluated by simulation. The simulated results showed a large improvement in the power factor control ability of the system if capacitor banks are used.

A possible solution to the problem associated with controlling the power factor at low active power levels is to decrease the voltage difference between consecutive taps. The number of capacitor banks can also be increased. By implementing, thus, smaller voltage steps and increasing the number of capacitor banks between consecutive tap changes, the reactive power control capability of the system is improved.

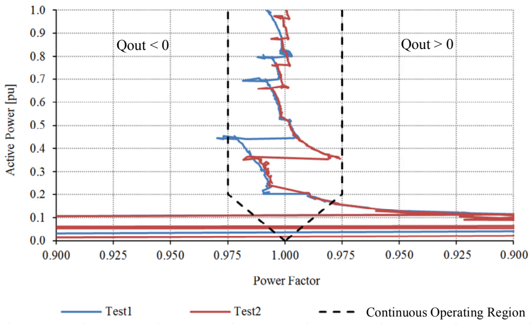


Fig. 19. Measured power factor at the grid connection point when using the OLTC transformer to control the reactive power output of the 15 kW SSG.

## VII. APPENDIX

TABLE 1. SSG VHDL-AMS MODEL PARAMETER VALUES

| Parameter | Value |
|---|---|
| Rated Voltage (Base) [V] | 400 |
| Rated Current (Base) [A] | 23 |
| Rated Frequency [Hz] | 50 |
| Poles | 40 |
| $L_{dr}$ [µH] | 0.127 |
| $L_{qr}$ [µH] | 0.09 |
| $R_r$ [µΩ] | 2.341 |
| $\lambda_{mr}$ [mWb] | 3.693 |
| $L_{ds}$ [mH] | 15 |
| $L_{qs}$ [mH] | 15 |
| $R_s$ [mΩ] | 380 |
| $\lambda_{ms}$ [Wb] | 1.0171 |
| $J_m$ [kg.m$^2$.rad$^{-2}$] | 10.0 |
| $J_t$ [kg.m$^2$.rad$^{-2}$] | 328.0 |

TABLE 2. TRANSFORMER VHDL-AMS MODEL PARAMETER VALUES

| Parameter | Value |
|---|---|
| Rated Voltage [V] | 400 |
| Rated Current [A] | 30 |
| Rated Frequency [Hz] | 50 |
| Rated Power [kVA] | 30 |
| R [mΩ] | 134 |
| L [µH] | 882 |

| Tap | 1 | 2 | 3 | 4 | 5 | 6 | 7 | 8 | 9 | 10 |
|---|---|---|---|---|---|---|---|---|---|---|
| Ratio | 1.2 | 1.1 | 1.0 | 0.95 | 0.9 | 085 | 0.8 | 0.75 | 0.7 | 0.65 |

TABLE 3. GRID VHDL-AMS MODEL PARAMETER VALUES

| Parameter | Value |
|---|---|
| Line-to-Line Voltage [V] | 400 |
| Frequency [Hz] | 50 |
| Line Resistance [mΩ] | 150 |
| Line Inductance [µH] | 477 |

## VIII. REFERENCES


[1] A. D. Hansen and H. a. L. H., "Market penetration of wind turbine concepts over the years," in *Proc. of the European Wind Energy Conference & Exhibition*, Milan, Italy, 2007.

[2] F. Spinato, P. Tavner, G. van Bussel and E. Koutoulakos, "Reliability of wind turbine subassemblies," in *Renewable Power Generation, IET*, December 2009.

[3] P. J. Tavnet, G. J. W. Van Bussel and F. Spinato, "Machine and Converter Reliabilities in Wind Turbines," in *Power Electronics, Machines and Drives, 2006. The 3rd IET International Conference on* , Mar. 2006.

[4] U. Hoffmann, P. Bouwer and M. Kamper, "Direct grid connection of a slip-permanent magnet wind turbine generator," *Energy Conversion Congress and Exposition (ECCE), 2011 IEEE,* pp. 2373-2380, 17-22 Sept. 2011.

[5] N. Jenkins, "Electrical Design of Wind Farms," in *Athens Power Tech, 1993. APT 93. Proceedings. Joint International Power Conference*, 5 - 8 Sep 1993.

[6] NERSA, September 2011. [Online]. Available: http://www.nersa.org.za.

[7] M. Heathcote and D. Franklin, The J & P Transformer Book, 12th ed., Oxford: Reed Educational and Professional Publishing Ltd, 1998.

[8] D. J. Rojers and T. C. Green, "A Hybrid Diverter Design for Distribution Level On-load Tap Changers," in *IEEE Energy Conversion Congress & Expo*, Atlanta, USA, 2010.

[9] P. Bouwer, J. Potgieter and M. Kamper, "Modelling and dynamic performance of a direct-drive direct-grid slip permanent magnet wind generator," *Electric Machines & Drives Conference (IEMDC), 2011 IEEE International,* pp. 137-142, 15-18 May 2011.

[10] L. H. Hansen, L. Helle, F. Blaabjerg, E. Ritchie, S. Munk-Nielsen, H. Bindner, P. Sørensen and B. Bak-Jensen, "Conceptual survey of Generators and Power Electronics for Wind Turbines," Roskilde, Denmark, December 2001.

[11] M. Elnashar, M. Kazerani, R. El Shatshat and M. Salama, "Comparative evaluation of reactive power compensation methods for a stand-alone wind energy conversion system," *Power Electronics Specialists Conference, 2008. PESC 2008. IEEE* , pp. 4539 - 4544 , 15-19 June 2008.